Supplementary Information for:

Climate change, fire return intervals and the growing risk of permanent forest loss in in boreal Eurasia

Arden L. Burrell[1,2*]
Qiaoqi Sun[3,4]
Robert Baxter[3]
Elena A. Kukavskaya[5]
Sergey Zhila[5]
Tatiana Shestakova[1]
Brendan M. Rogers[1]
Kirsten Barrett[2]

1. Woodwell Climate Research Center, Falmouth, MA, United States of America
2. Centre for Landscape and Climate Research, School of Geography, Geology and Environment, University of Leicester, University Road, LE1 7RH, UK
3. Department of Biosciences, University of Durham, Upper Mountjoy, South Road, Durham, DH1 3LE, United Kingdom.
4. College of Wildlife and Protected Area, Northeast Forestry University, 26 Hexing Road, Harbin 150040, China
5. V.N. Sukachev Institute of Forest of the Siberian Branch of the Russian Academy of Sciences - separate subdivision of the FRC KSC SB RAS, 660036 Russian Federation, Krasnoyarsk, Akademgorodok 50/28.

*Corresponding author

Email: aburrell@woodwellclimate.org

This PDF file includes:

Text 1

Figures S1 to S12

1. Assessing the accuracy of RS BA products

1.1. Method

Unlike boreal forests in North America and Scandinavia, the Russian boreal forest has a well-documented lack of site-level burn scar mapping that can be used to validate BA products (Burrell et al., 2021). This is especially true in parts of the former Soviet Union where, in some locations, the memory of individual foresters constitutes the only records of fires.

To assess the BA products, we estimated site-level fire histories at 50 existing field sites located in southern Siberia (Barrett et al., 2020) using Google Earth Engine to identify available Landsat images. For each site a time lapse video was built showing the R-G-B scenes as well as near infrared (NIR)-R-G and shortwave infrared (SIR)-NIR-R false colour composites. We used these videos to record every fire or disturbance event at the site, as well as within a 1 km-by-1 km bounding box around each site. To reduce the risk of user-error, every site was assessed by at least two people independently. Examples of a burn in these images are included in Supplementary Figure 1. We compared this user generated fire history with the BA products and scored the products using the following criteria: Correct Detection (CD) is a burn that is apparent in both the user generated and BA product (±1 year to account for gaps in the Landsat record). A Spatial Underestimation (SU) is when the BA product detects a fire in the 1 km x 1 km, but not in the pixel that includes the site, whilst the user generated fire history has the fire impacting the site. A Spatial Overestimation (SO) is the opposite of a Spatial Underestimation, with the manual fire history recording a fire in the box but not impacting the site, whilst the BA product detects a fire disturbance at the site. A False Negative (FN) represents a fire in the manual fire history but not in the BA data. A False Positive (FP) represents a fire in the BA that could not be observed in the manual fire history. A similar approach was used to assess HansenGFC, though all stand loss disturbances were considered, and for HansenGFC-MAF, in which case only stand loss driven by fire events, was included. GFED4 was not assessed because its spatial resolution is too coarse for site-level accuracy assessments.

The main limitation to our time-series based approach to identifying burned areas is that, whilst it is easy to detect stand-replacing fires in the Landsat images because the impacts are apparent for years after the actual burn, gaps in the Landsat record mean it is easy to miss low severity understory or grassland fires. This is a potential problem because forests that are regenerating after a stand-replacing fire are dominated by grasses (Kukavskaya et al., 2014) and are spectrally similar to grasslands. As such, our ability to assess Correct Detections (CD) of burned area and False Negatives (FN) is much higher than our ability to assess False Positives (FP), with a portion of the FP's we observe likely being correct detections that could not be seen in the available Landsat images due to low fire severity.

1.2. Results and Discussion

We find that all three BA products have low accuracy, with the most accurate dataset (FireCCI51) only correctly detecting fires *ca*. 34 % of the time (Supplementary Figure 2). This is in line with previous assessments of the accuracy of BA products that have shown that, whilst performance in boreal forest is better than other ecozones (Humber et al., 2019), the rates of both omission (False Negative) and commission (False Positive) errors are generally high, and omissions exceed commissions in most studies (Brennan et al., 2019; Giglio et al., 2018; Humber et al., 2019; Lizundia-Loiola et al., 2020).

While the low accuracy of BA products is a problem that requires further research (Humber et al., 2019), it only impacts our ability to use FRI to infer the risk of permanent forest loss if the BA datasets have a significant positive bias. We find that all the BA products tend to underestimate the spatial extent of burns. MCD64A1 and CGLS-BA also have a net omission bias which suggests that the FRI's calculated using these datasets underestimate the risk of FRI-driven forest loss. While we could not assess the accuracy of GFED4 directly, it detects less burnt area in the Eurasian forest than MCD64A1. Because our results and previous studies have shown MCD64A1 to have a net omission bias (Humber et al., 2019), we therefore assume GFED4 also has a net omission bias and thereby overestimates FRI. This is in line with previous assessments of the accuracy of BA products that have shown that, whilst performance in boreal forest is better than other ecozones (Humber et al., 2019), the rates of both omission (False Negative) and commission (False Positive) errors are generally high, and omissions exceed commissions in most studies (Brennan et al., 2019; Giglio et al., 2018; Humber et al., 2019; Lizundia-Loiola et al., 2020).

In contrast to MCD64A1 and CGLS-BA, the false positive rate of FireCCI51 exceeds the false negative rate. Although this does suggest that the FRI calculated from FireCCI51 may overestimate the risk of permanent forest loss, our method used to assess the accuracy of the datasets is likely to overestimate the rate of False Positives. The same limitation in our assessment method may also explain why HansenGFC and HansenGFC-MAF have unexpectedly high rates of commission error (Krylov et al., 2014). Previous studies have shown that MCD64A1 underestimates BA in boreal Eurasia and that FireCCI51 corrects for this bias whilst still retaining a net omission bias (Humber et al., 2019; Lizundia-Loiola et al., 2020). Taken together, our results suggest that the FRI is a useful proxy for assessing RF risk in boreal forests. They also suggest that FRI calculated using MCD64A1 and FireCCI51 are likely the most accurate, with MCD64A1 representing a lower bound on burnt area and FireCCI51 likely closest to the actual FRI.

CGLS-BA has the lowest accuracy (Supplementary Figure 2) and has significant spatial differences in estimated FRI (Figure 2). The differences in the south-eastern portion of the study are unsurprising because CGLS-BA has a much shorter record and cannot capture fires during spring or autumn north of 51°N (Smets et al., 2017). This is problematic because in south-eastern Siberia the fire season starts as early as March (Feurdean et al., 2020; Hayasaka et al., 2020; Shvetsov et al., 2019). However, this cannot explain why CGLS-BA has much shorter FRI's in north-western Siberia. Previous assessments of BA accuracy noted the tendency for CGLS-BA to overestimates burns in this region (Humber et al., 2019). These same issues also impact the ML model. Whilst there is generally good agreement between different models regarding feature importance, the CGLS-BA based model diverges from the other models with much lower permutation importance for winter and spring temperature (Figure 7). This is particularly interesting because winter and early spring climate is strongly tied to spring fire events (Feurdean et al., 2020; Kim et al., 2020), which CGLS-BA cannot detect. This supports the idea that permutation importance is more accurately capturing the real variable importance, a result which is expected given previous studies that have compared the methods (Wei et al., 2015).

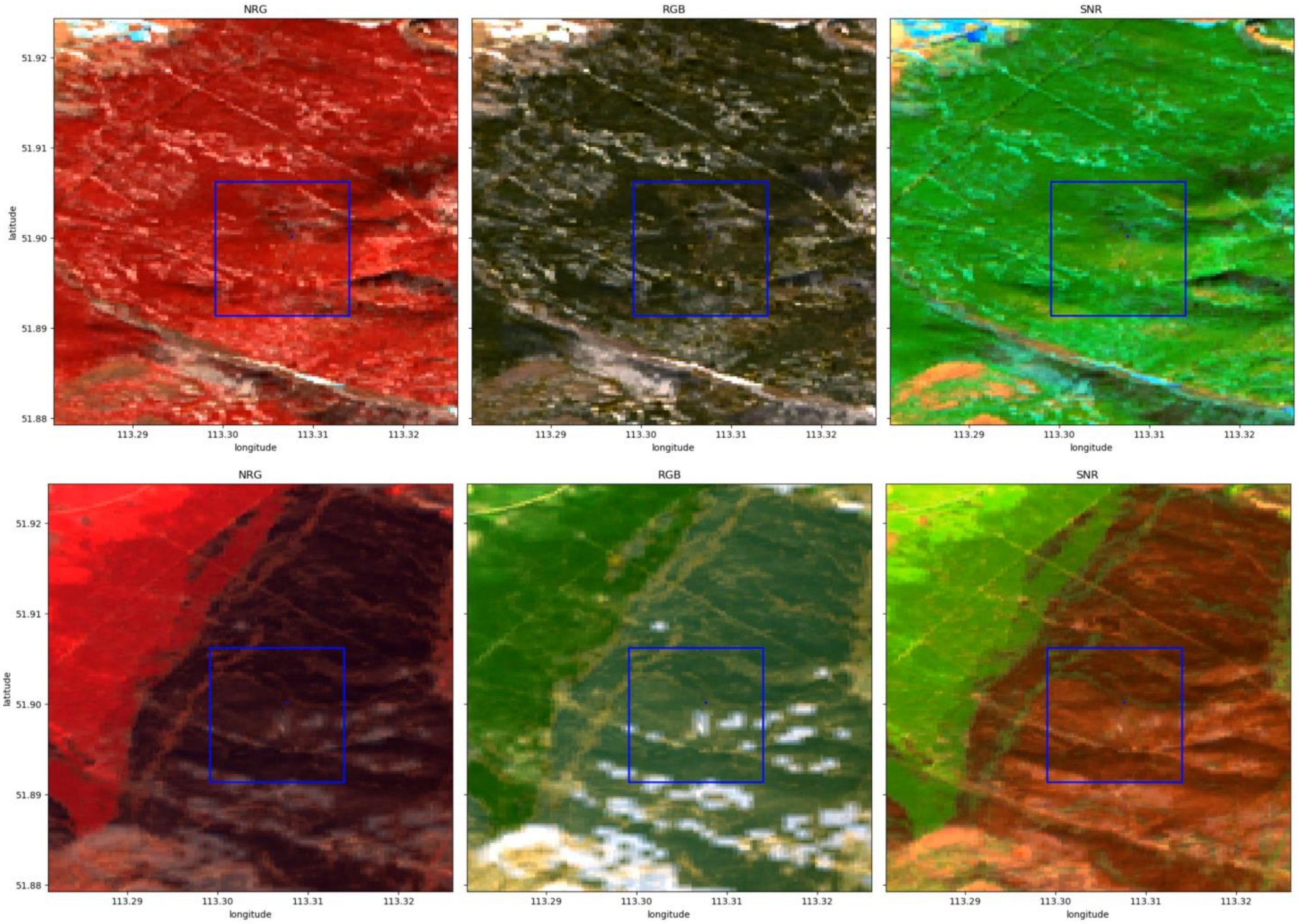

Figure S1 - Example of a 2015 burn at a test site. *NGR is a Near Infrared, Red, Green false-colour image. RGB is the true colour image and SNR is the Shortwave Infrared, Near Infrared, red false-colour image. The blue box is a 1 kmx1 km area around the site that matches the exact grid of the BA datasets and the blue dot in the box is the location of the site. The top row of images are from 2015-03-18 and the bottom row are from 2015-09-08.*

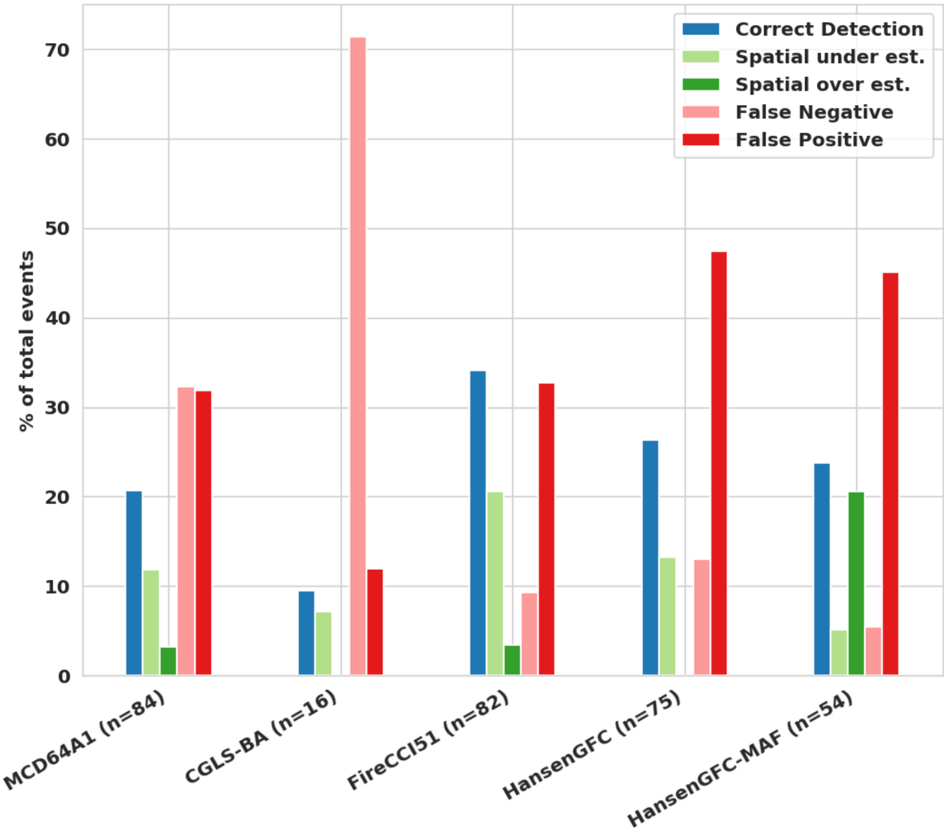

Figure S2 Accuracy of BA and forest loss products *at sites in the Zabaikal region. The BA products are compared to a manually generated fire history constructed at each site using the entire Landsat archive. An event is a burn that is observed in the Landsat record and/or the BA product.*

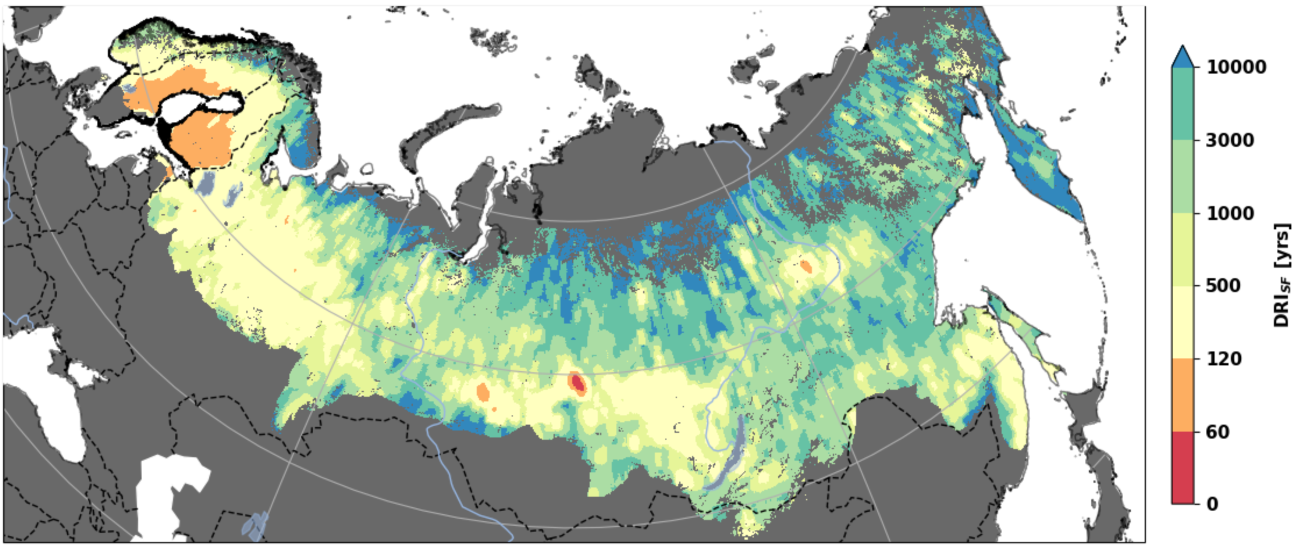

Figure S3 – Disturbance return interval. *The DRI sans fires (DRI$_{SF}$) calculated by removing the forest attributable to fire (HansenGFC-AFM) from the DRI (HansenGFC).*

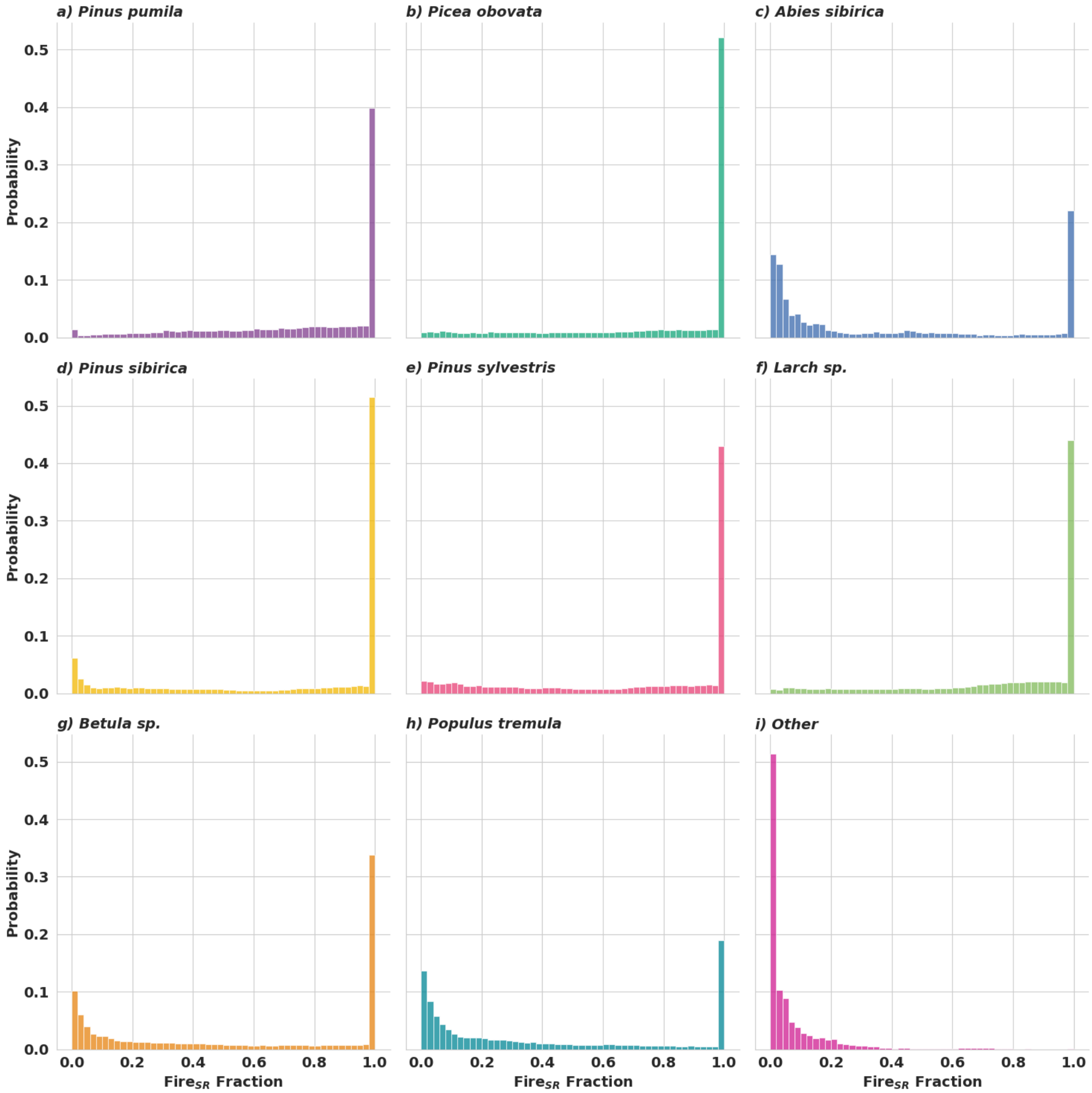

Figure S4 Stand-replacing fire fraction. *Binned probabilty distribution histogram of the stand-replacing fire fraction (FireCCI5.1 mean annual burn fraction / HansenGFC-MAF mean annual burn fraction) for the dominant tree species. Areas where tree species data were unavilable, or where FireCCI5.1 FRI> 10,000 yrs, were excluded.*

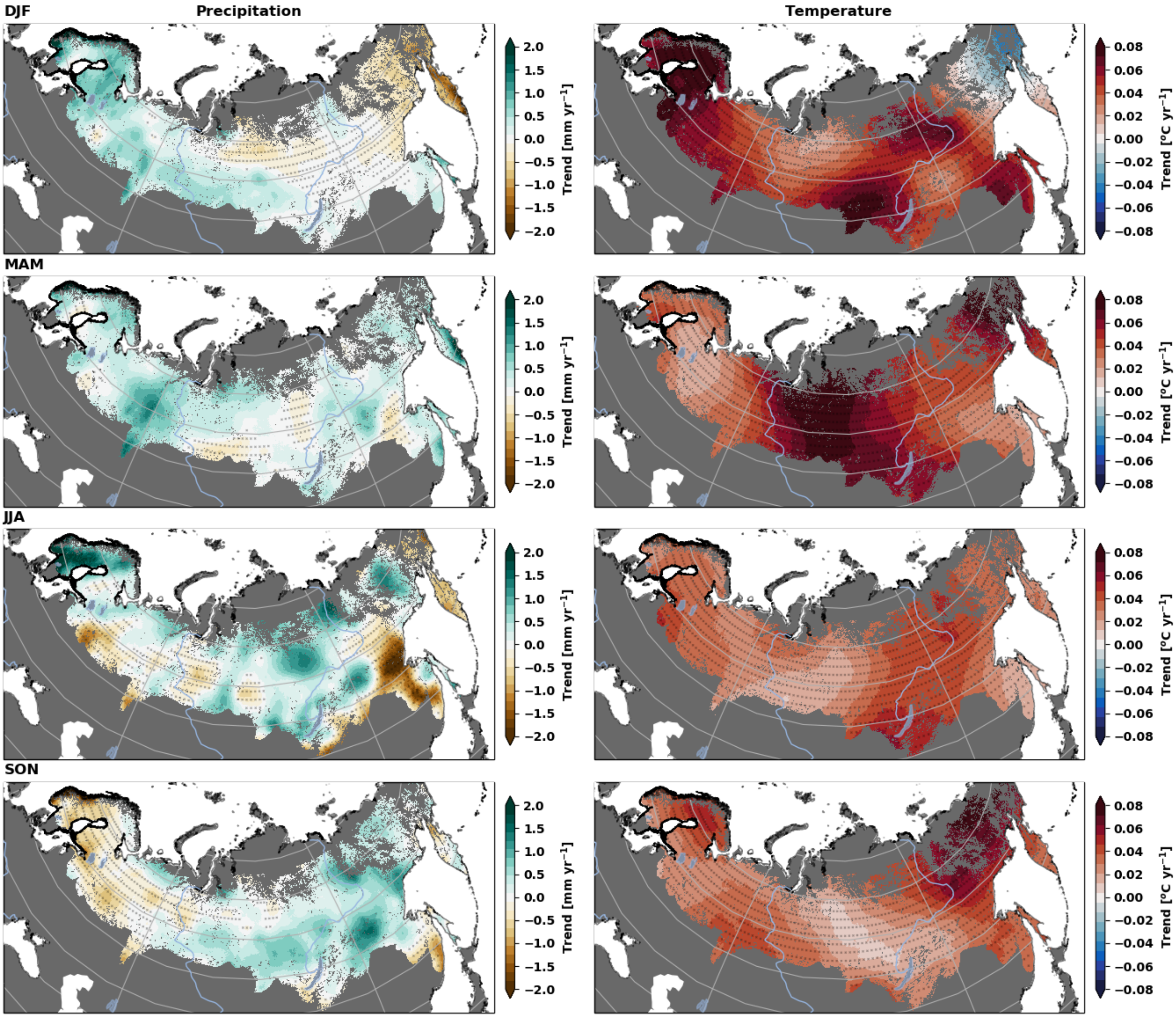

Figure S5 - Climate change driven trends *in seasonal accumulated Precipitation and mean Temperature for the period 1985 to 2015. This figure uses the meteorological seasons December January February (DJF), March April May (MAM), June July August (JJA) and September October November (SON). Non-boreal forest ecosystems are masked in grey and the stippling indicates statistical significance (α_{FDR} = 0.10). Data: TerraClimate (Abatzoglou et al., 2018)*

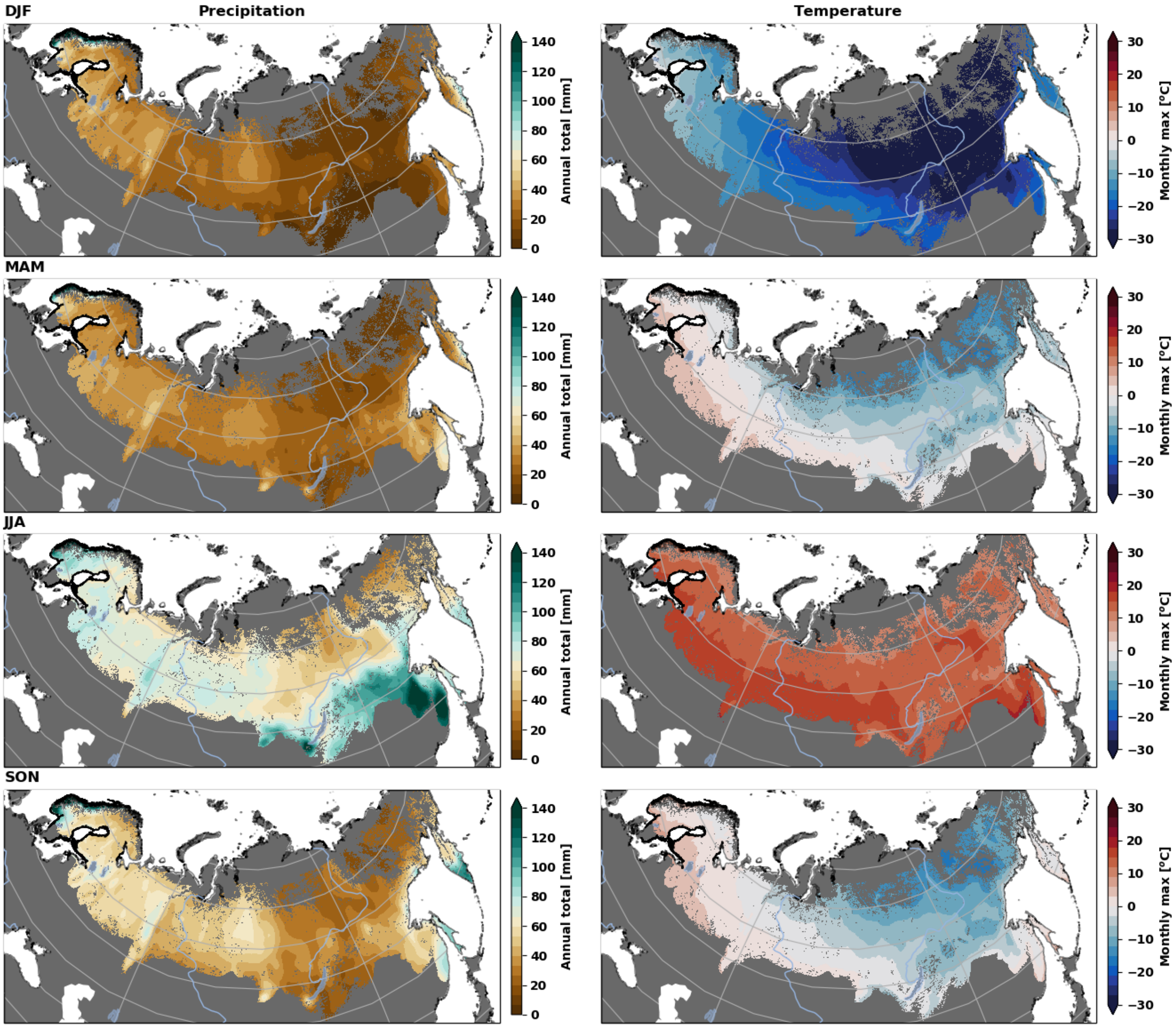

Figure S6 - Mean seasonal climatology *for the period 1985 to 2015. This figure uses the meteorological seasons December January February (DJF), March April May (MAM), June July August (JJA) and September October November (SON). Non-boreal forest ecosystems are masked in grey. Data: TerraClimate (Abatzoglou et al., 2018)*

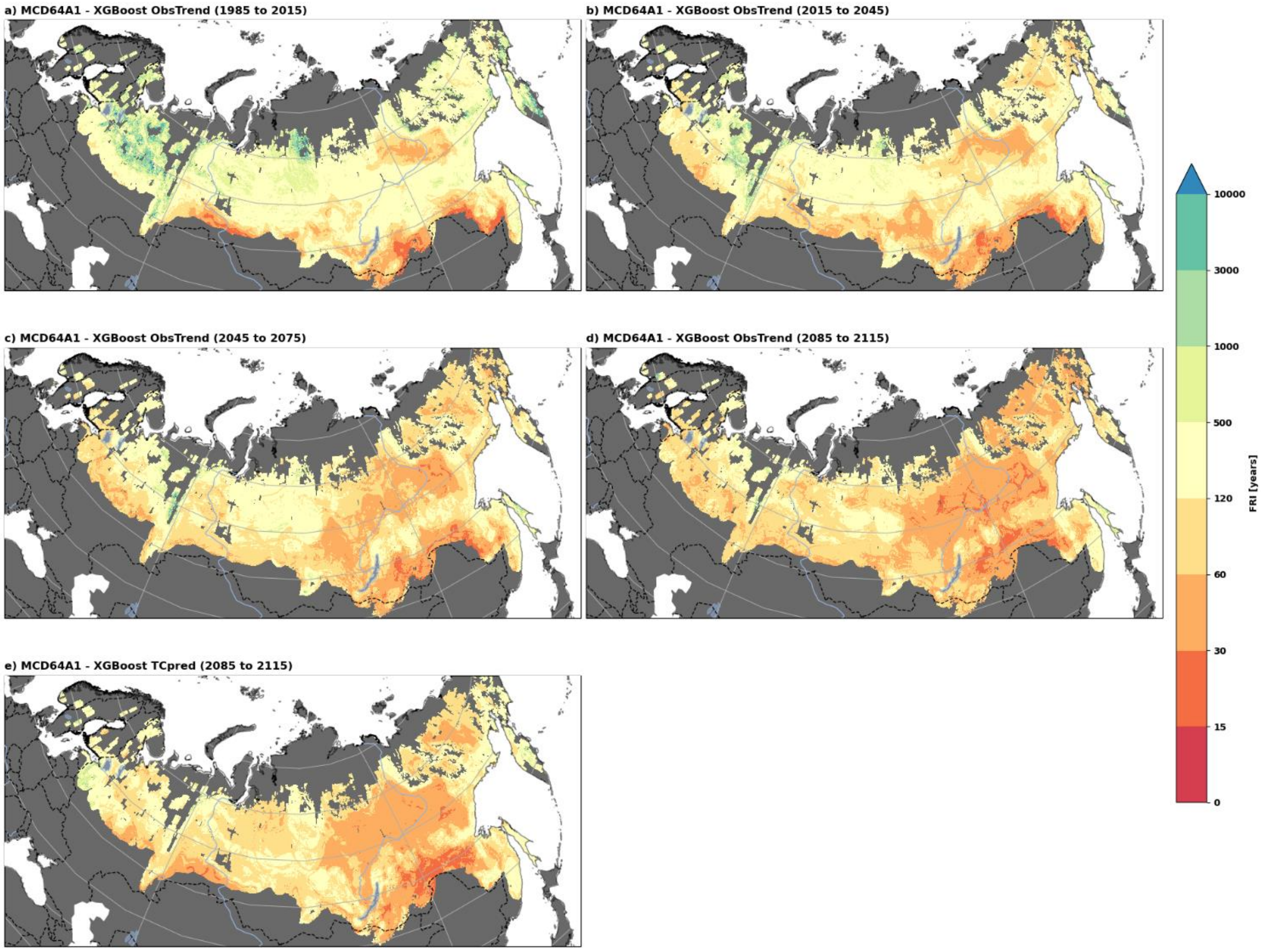

Figure S7 - Maps of the predicted FRI *based on current climate trend, XGBoost ML and MCD64A1 FRI data. TCpred is the Terraclimate prediction for a 4^{0}C warmer world which is approximately SSP3-7.0 2085 – 2115. Non-boreal forest ecosystems are masked in grey.*

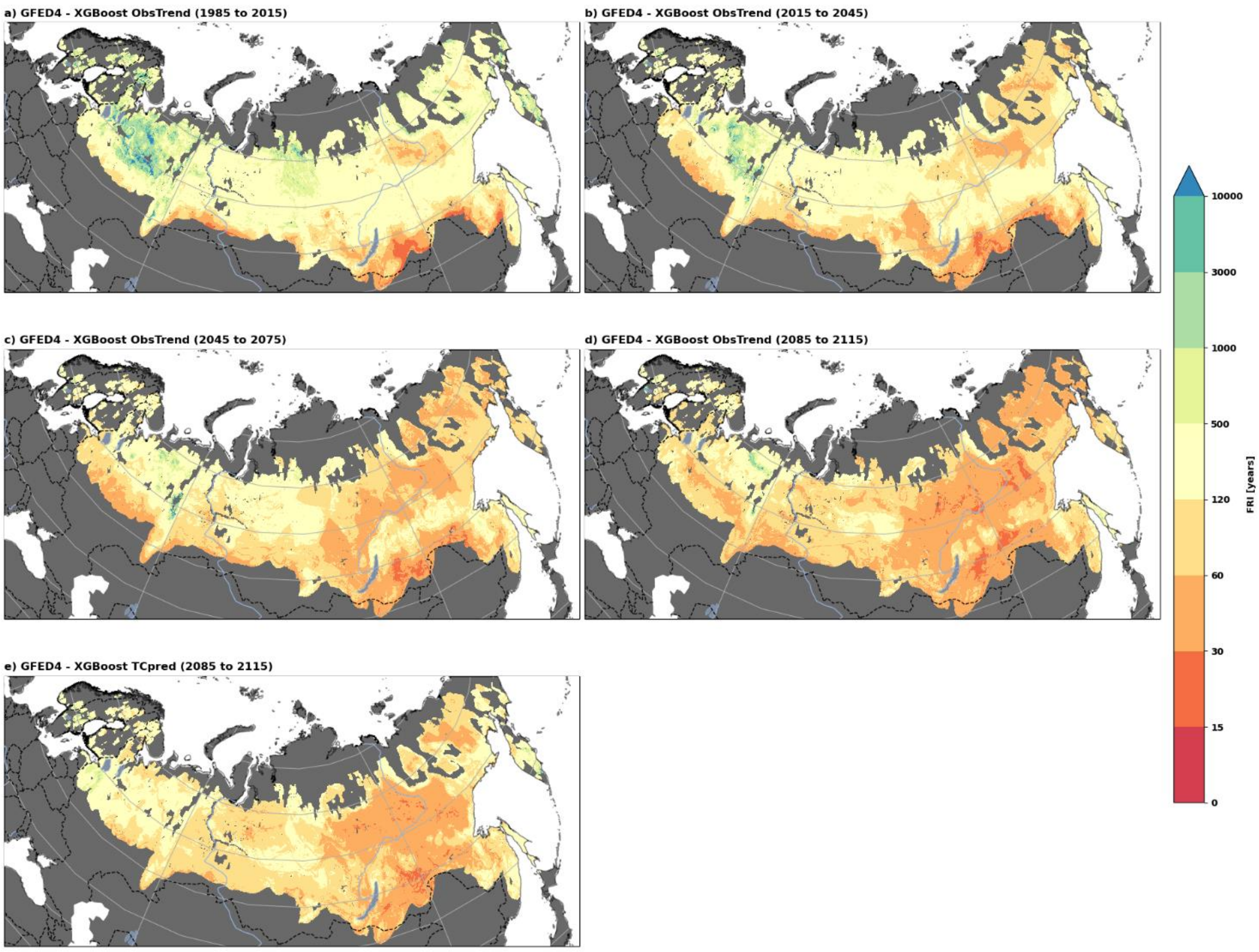

Figure S8 -Maps of the predicted FRI *based on current climate trend, XGBoost ML and GFED FRI data. TCpred is the Terraclimate prediction for a 4⁰C warmer world which is approximately SSP3-7.0 2085 – 2115. Non-boreal forest ecosystems are masked in grey.*

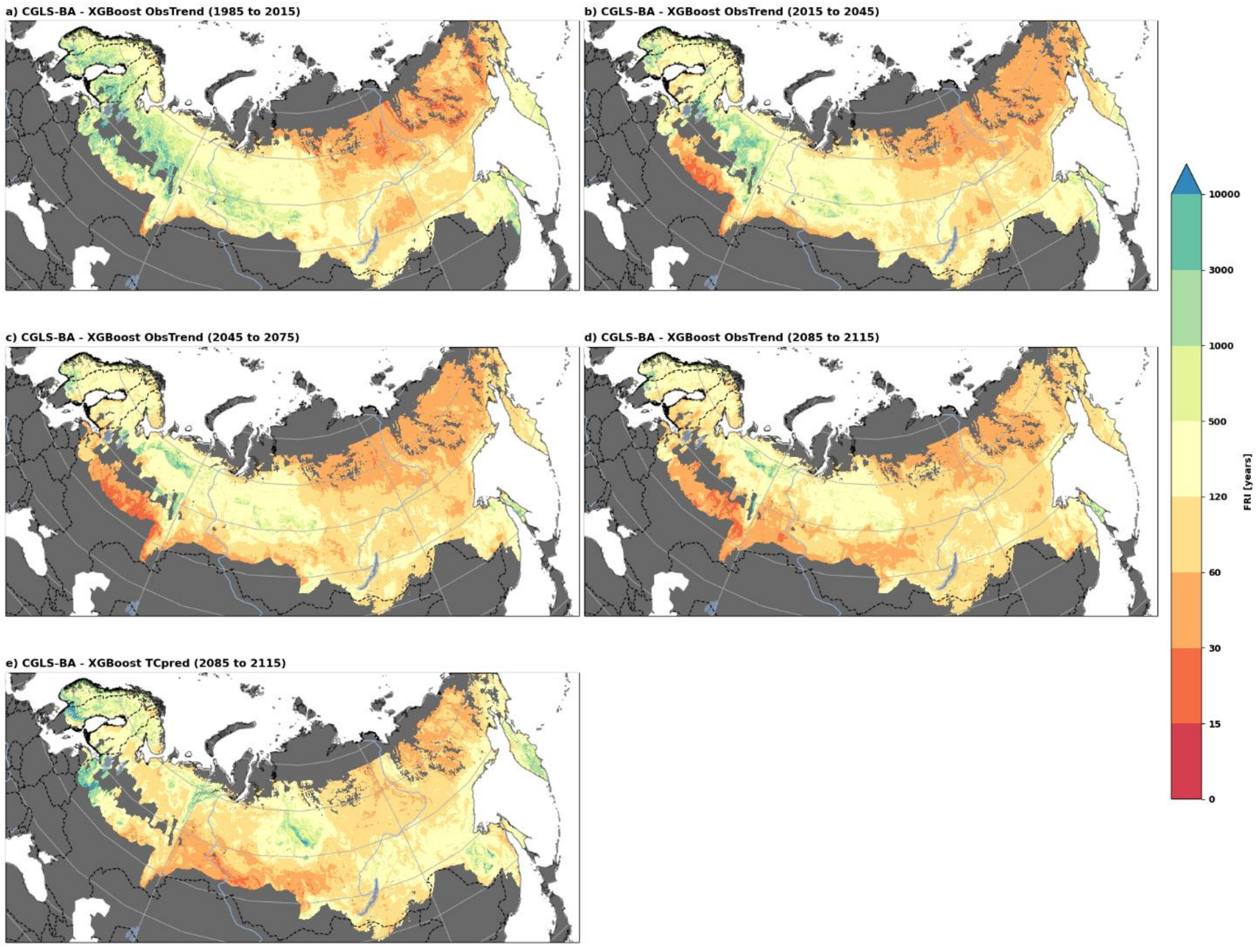

Figure S9 - Maps of the predicted FRI *based on current climate trend, XGBoost ML and CGLS-BA FRI data. TCpred is the Terraclimate prediction for a 4^0C warmer world which is approximately SSP3-7.0 2085 – 2115. Non-boreal forest ecosystems are masked in grey.*

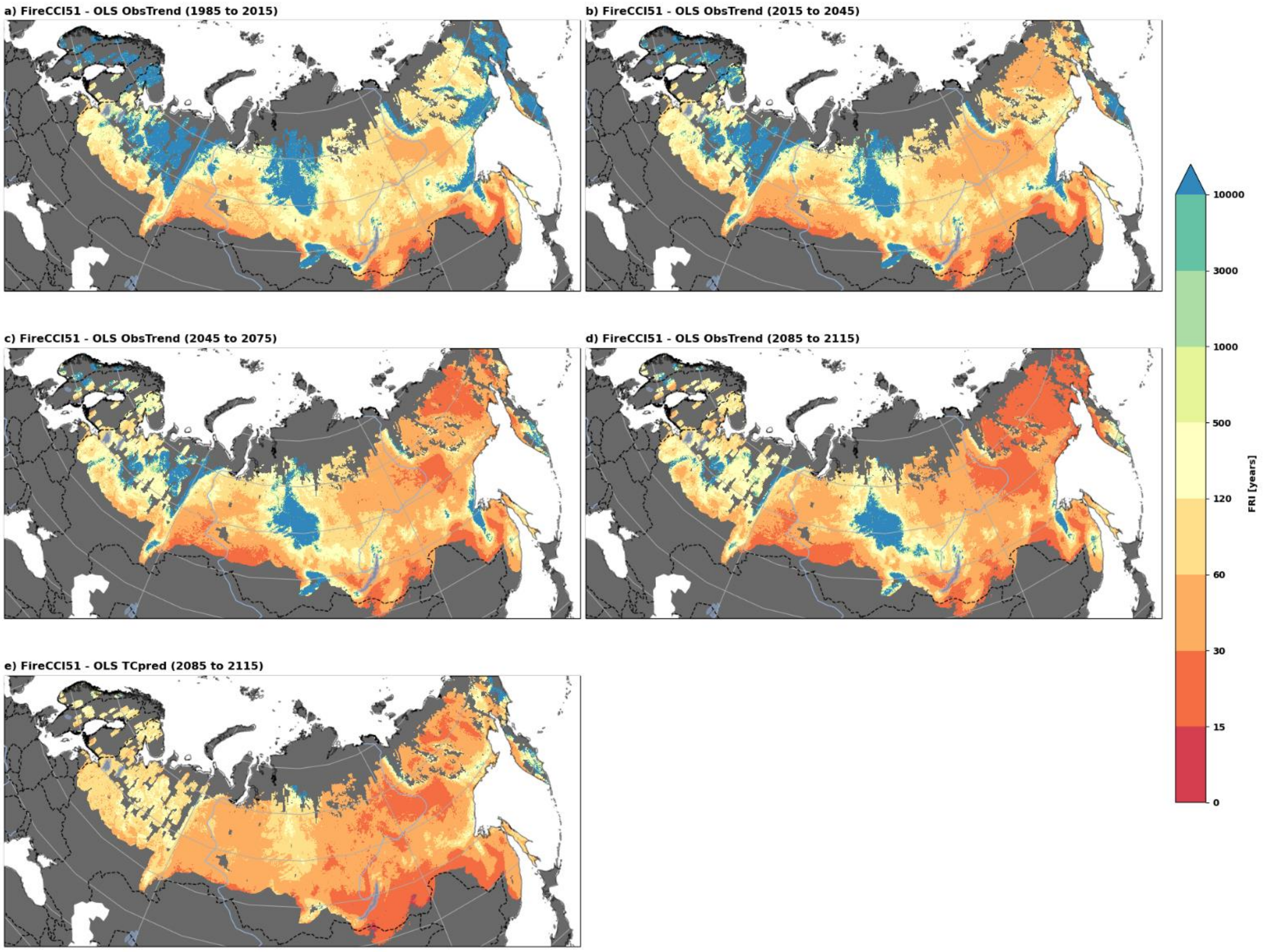

Figure S10 - Maps of the predicted FRI *based on current climate trend, OLS and FireCCI51 FRI data. TCpred is the Terraclimate prediction for a 4^0C warmer world which is approximately SSP3-7.0 2085 – 2115. Non-boreal forest ecosystems are masked in grey.*

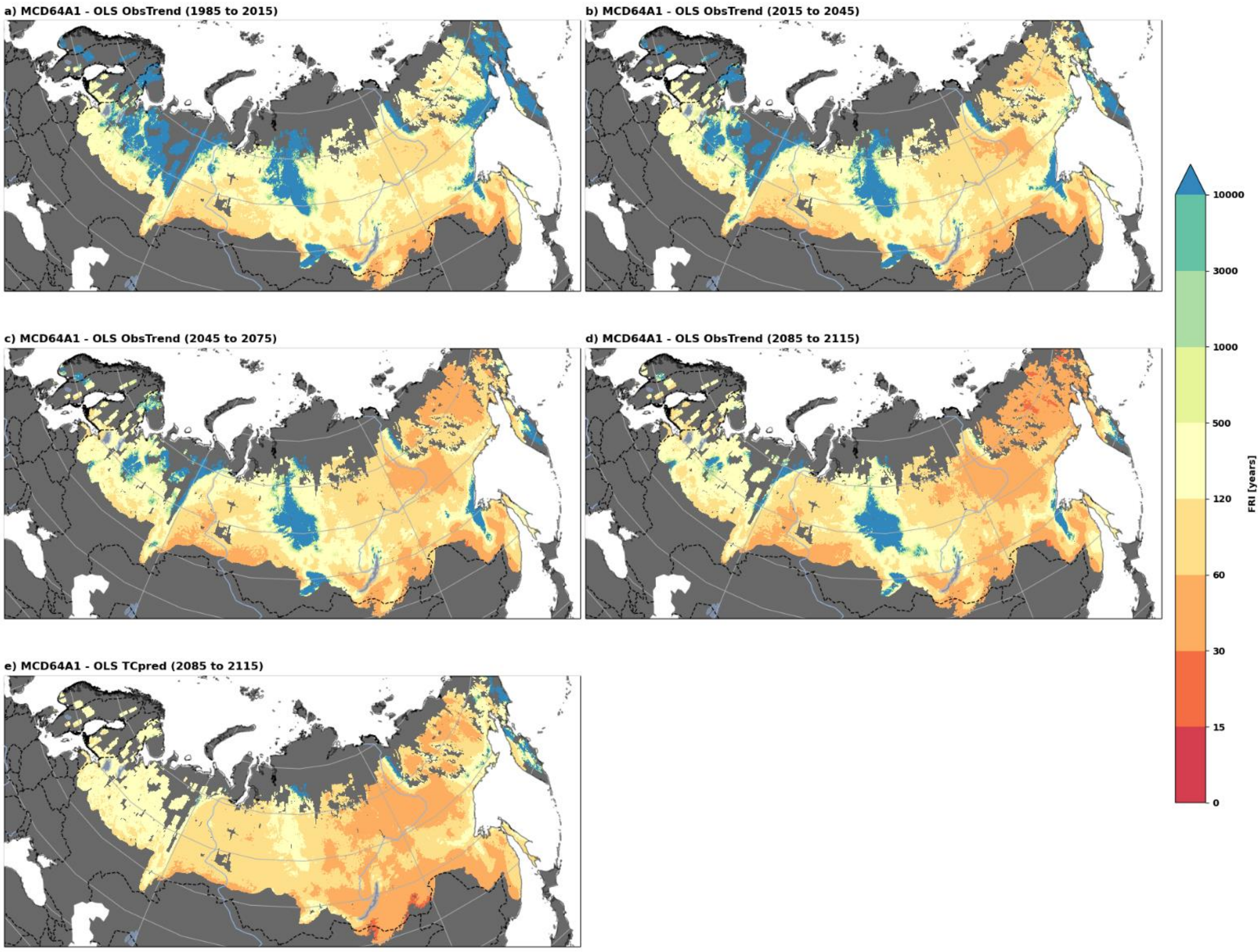

Figure S11 - Maps of the predicted FRI *based on current climate trend, OLS and MCD64A1 FRI data. TCpred is the Terraclimate prediction for a 4^{0}C warmer world which is approximately SSP3-7.0 2085 – 2115. Non-boreal forest ecosystems are masked in grey.*

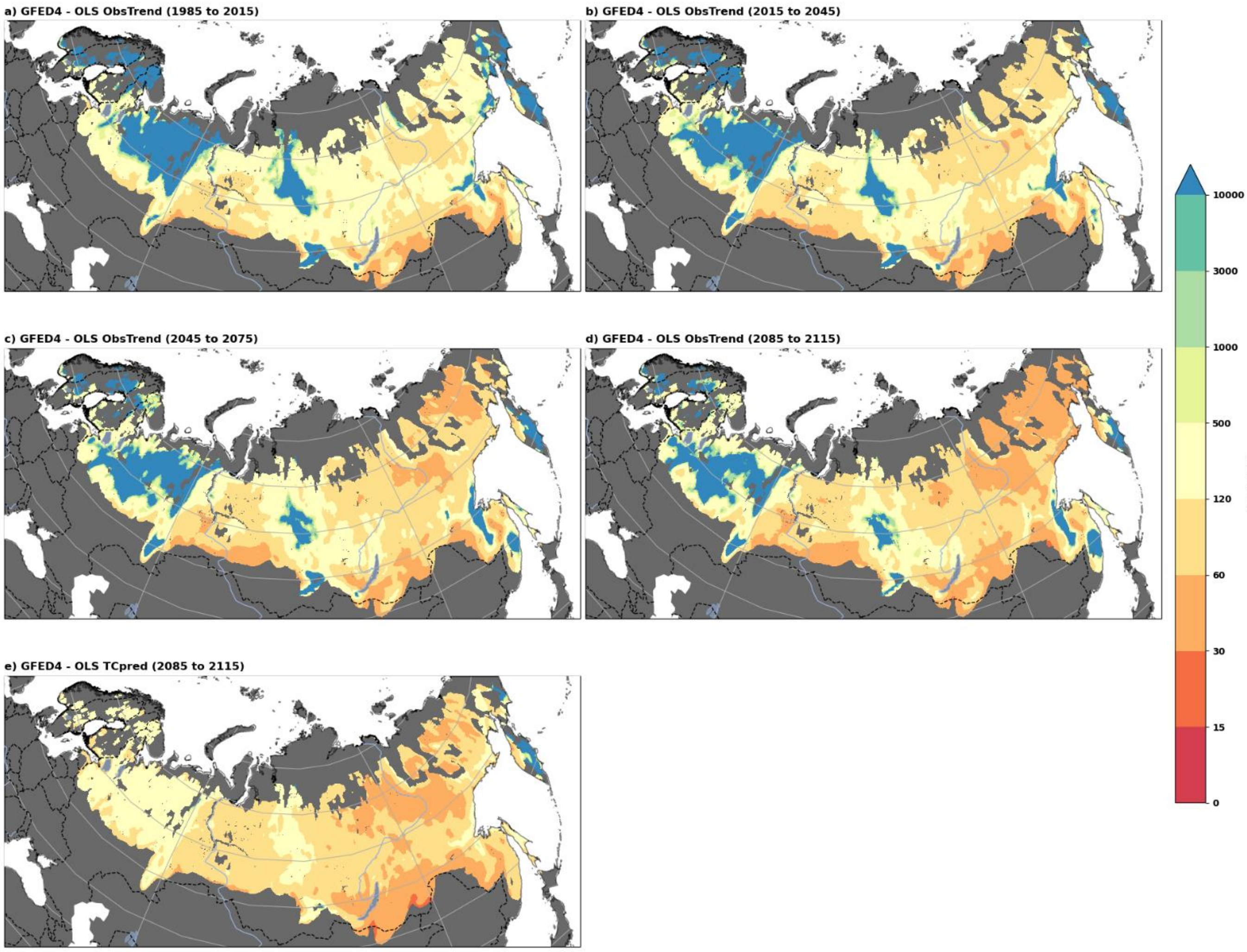

Figure S12 - Maps of the predicted FRI *based on current climate trend, OLS and GFED4 FRI data. TCpred is the Terraclimate prediction for a 4^{0}C warmer world which is approximately SSP3-7.0 2085 – 2115. Non-boreal forest ecosystems are masked in grey.*

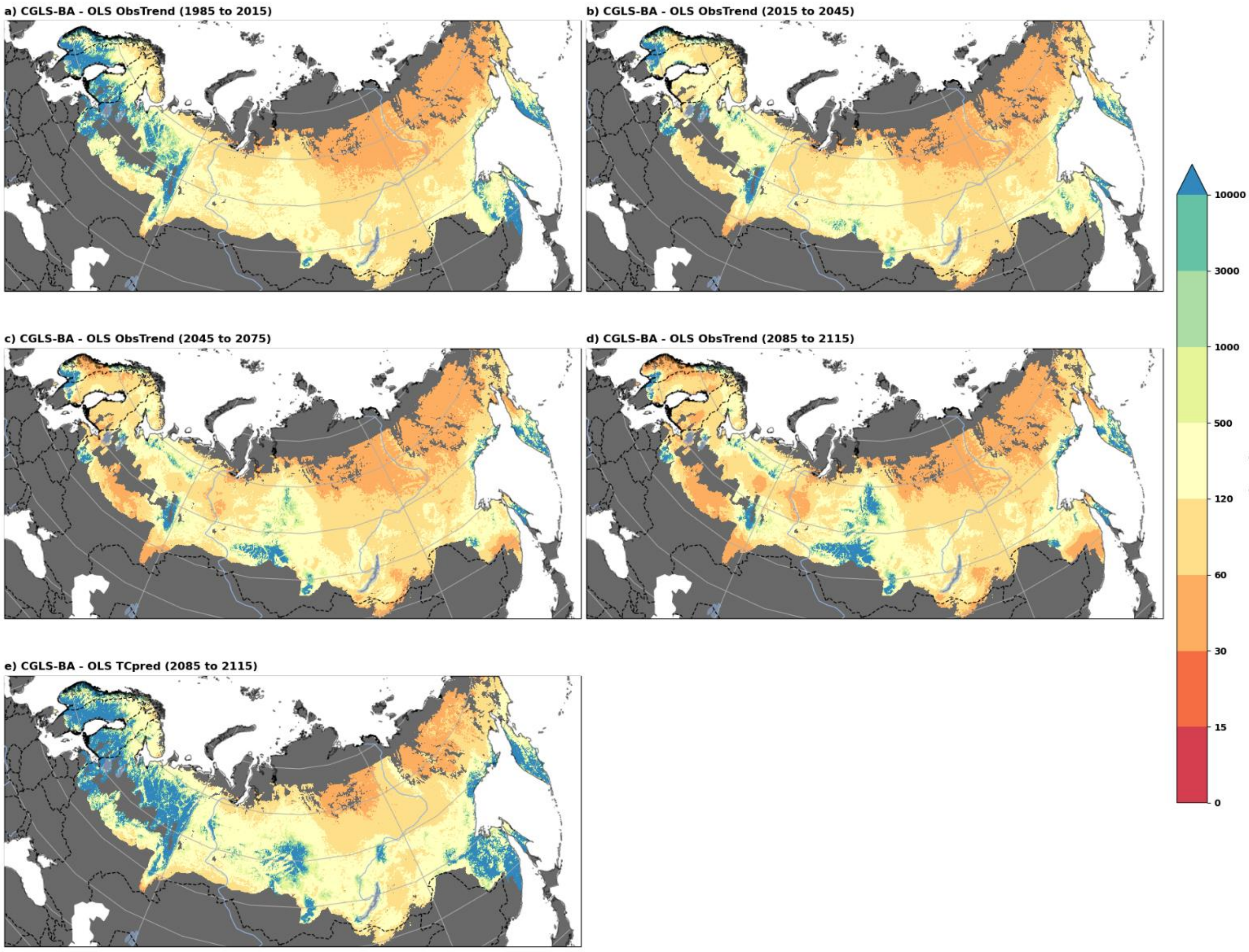

Figure S13 - Maps of the predicted FRI *based on current climate trend, OLS and CGLS-BA FRI data. TCpred is the Terraclimate prediction for a 4^{0}C warmer world which is approximately SSP3-7.0 2085 – 2115. Non-boreal forest ecosystems are masked in grey.*

References

Abatzoglou, J.T., Dobrowski, S.Z., Parks, S.A., Hegewisch, K.C., 2018. TerraClimate, a high-resolution global dataset of monthly climate and climatic water balance from 1958–2015. Sci. Data 5, 170191. https://doi.org/10.1038/sdata.2017.191

Barrett, K., Baxter, R., Kukavskaya, E., Balzter, H., Shvetsov, E., Buryak, L., 2020. Postfire recruitment failure in Scots pine forests of southern Siberia. Remote Sens. Environ. 237, 111539. https://doi.org/10.1016/j.rse.2019.111539

Brennan, J., Gómez-Dans, J.L., Disney, M., Lewis, P., 2019. Theoretical uncertainties for global satellite-derived burned area estimates. Biogeosciences 16, 3147–3164. https://doi.org/10.5194/bg-16-3147-2019

Burrell, A.L., Kukavskaya, E.A., Baxter, R., Sun, Q., Barrett, K., 2021. Post-fire recruitment failure as a driver of forest to non-forest ecosystem shifts in boreal regions, in: Ecosystem Collapse and Climate Change, Ecological Studies. Springer International Publishing.

Feurdean, A., Florescu, G., Tanţău, I., Vannière, B., Diaconu, A.-C., Pfeiffer, M., Warren, D., Hutchinson, S.M., Gorina, N., Gałka, M., Kirpotin, S., 2020. Recent fire regime in the southern boreal forests of western Siberia is unprecedented in the last five millennia. Quat. Sci. Rev. 244, 106495. https://doi.org/10.1016/j.quascirev.2020.106495

Giglio, L., Boschetti, L., Roy, D.P., Humber, M.L., Justice, C.O., 2018. The Collection 6 MODIS burned area mapping algorithm and product. Remote Sens. Environ. 217, 72–85. https://doi.org/10.1016/j.rse.2018.08.005

Hayasaka, H., Sokolova, G.V., Ostroukhov, A., Naito, D., 2020. Classification of Active Fires and Weather Conditions in the Lower Amur River Basin. Remote Sens. 12, 3204. https://doi.org/10.3390/rs12193204

Humber, M.L., Boschetti, L., Giglio, L., Justice, C.O., 2019. Spatial and temporal intercomparison of four global burned area products. Int. J. Digit. Earth 12, 460–484. https://doi.org/10.1080/17538947.2018.1433727

Kim, J.-S., Kug, J.-S., Jeong, S.-J., Park, H., Schaepman-Strub, G., 2020. Extensive fires in southeastern Siberian permafrost linked to preceding Arctic Oscillation. Sci. Adv. 6, eaax3308. https://doi.org/10.1126/sciadv.aax3308

Krylov, A., McCarty, J.L., Potapov, P., Loboda, T., Tyukavina, A., Turubanova, S., Hansen, M.C., 2014. Remote sensing estimates of stand-replacement fires in Russia, 2002–2011. Environ. Res. Lett. 9, 105007. https://doi.org/10.1088/1748-9326/9/10/105007

Kukavskaya, E.A., Ivanova, G.A., Conard, S.G., McRae, D.J., Ivanov, V.A., 2014. Biomass dynamics of central Siberian Scots pine forests following surface fires of varying severity. Int. J. Wildland Fire 23, 872–886. https://doi.org/10.1071/WF13043

Lizundia-Loiola, J., Otón, G., Ramo, R., Chuvieco, E., 2020. A spatio-temporal active-fire clustering approach for global burned area mapping at 250 m from MODIS data. Remote Sens. Environ. 236, 111493. https://doi.org/10.1016/j.rse.2019.111493

Shvetsov, E.G., Kukavskaya, E.A., Buryak, L.V., Barrett, K., 2019. Assessment of post-fire vegetation recovery in Southern Siberia using remote sensing observations. Environ. Res. Lett. 14, 055001. https://doi.org/10.1088/1748-9326/ab083d

Smets, B., Tansey, K., Wolfs, D., Jacobs, T., 2017. PRODUCT USER MANUAL BURNED AREA AND SEASONALITY COLLECTION 300M VERSION 1.

Wei, P., Lu, Z., Song, J., 2015. Variable importance analysis: A comprehensive review. Reliab. Eng. Syst. Saf. 142, 399–432. https://doi.org/10.1016/j.ress.2015.05.018